2024 Tenth Indian Control Conference (ICC)
9 - 11 December, 2024
IISER Bhopal, India

Curved Platooning of Position-Controlled Vehicles with Two Communication Topologies

Rintu Bhaskar, Pankaj Wahi, and Ramprasad Potluri

***Abstract*—This paper addresses vehicle platooning on curved path or curved platooning and presents an algorithmic solution for platooning homogeneous position-controlled vehicles (PCVs) under two communication topologies: leader-following (LF) and predecessor-following (PF). Most existing works present curved platooning with constant speed. On the other hand, this work demonstrates curved platooning with varying speeds. In this paper, all the follower vehicles receive the lead vehicle's communicated actual trajectory, i.e., its actual position and orientation, for platooning with the LF topology. In LF topology, a follower vehicle remains unaware of its preceding vehicle's maneuver and PF topology overcomes this limitation. Therefore, this paper investigates platooning with PF topology using the reference as well as the actual trajectory of the preceding vehicle in two separate approaches. In all the approaches, a follower vehicle creates a virtual trail of the lead or the preceding vehicle by storing the communicated information from the respective vehicles. An algorithm on the follower vehicle uses the virtual trail and finds the follower vehicle's reference position and orientation on that trail, maintaining a constant inter-vehicle distance. This work compares the applicability of the algorithmic solutions with the LF and PF topologies and presents the simulation results.**

I. Introduction

An automated vehicle platoon improves traffic flow and road safety by reducing the inter-vehicle distance and the chances of accidents caused by driver's fault. An automated platoon is a train of vehicles where the follower vehicles automatically follow the lead vehicle [1]–[3]. Vehicle platooning on a straight path involves controlling the follower vehicle's longitudinal motion and is well-researched using cooperative adaptive cruise control. However, vehicle platooning on a curved path or curved platooning is still emerging and challenging as it involves simultaneous control of the follower vehicle's longitudinal and lateral motions. Existing curved platooning solutions use look-down or look-ahead approaches. [4], [5].

In the look-down approach, each follower vehicle (FV) looks down at the road centerline and tracks that centerline independently for lateral following [4]. Therefore, it requires a structured road, limiting its application. The look-ahead approach overcomes this limitation, and an FV tries to follow the lead vehicle (LV) at a look-ahead distance with vision-based approach [4], [6]–[8] and trajectory-based approach [3], [5], [9], [10]. In the vision-based approach, sensors, such as radar, lidar, and camera, measure the lateral and longitudinal deviation between the FV and its preceding vehicle (PV) [4], [6]. In the trajectory-based approach, an FV follows the trail of the LV or the PV [7]. The present work uses a trajectory-based curved platooning approach, and the proposed algorithmic solution works for a platoon on homogeneous PCVs.

Existing curved platooning solutions use constant speed motion [3]–[8] or near constant speed motion [9], [10] on the curve. However, in practice, the curvature of a road varies, and therefore, the speed needs to be varied. The present work offers curved platooning of PCVs with varying speeds under the LF and PF communication topologies.

The present work is an extension of the work [11], which proposes an algorithmic solution for curved platooning of homogeneous PCVs with constant distance spacing and LF topology. In [11], the LV communicates its reference trajectory (i.e., reference position and orientation) to all the FVs, and the algorithm helps an FV follow the LV's reference path. While following the LV's reference path, an FV remains unaware of the LV's actual path and may deviate from it. To overcome this drawback, as the primary contribution, the present paper modifies the algorithm in [11] and presents curved platooning using the LV's actual trajectory (i.e., output position and orientation) instead of its reference trajectory.

The LF topology has a drawback: an FV remains unaware of any emergency maneuver of its PV. Platooning with the PF topology overcomes this drawback. As a secondary contribution, this paper modifies the algorithm in [11] to use the PF topology for platooning. Here, the PV communicates its reference trajectory and actual trajectory to its immediate FV for platooning in two separate approaches. This work compares the applicability of the algorithmic solution for curved platooning with the LF and PF topologies in simulation.

In simulation, this paper considers a four-wheel independent steering four-wheel independent drive (4WIS4WID) PCV developed in [12] to demonstrate curved platooning with the LF and PF topologies. In curved platooning using the actual trajectory of the LV and PV, the path-tracking errors degrade the platoon's performance. This work replaces the PD path-tracking controller (PTC) of 4WIS4WID PCV in [12] with a PID PTC that reduces errors and improves performance.

This paper is organized as follows. Section II briefly describes the algorithmic solution for curved platooning with

The first two authors are with the Nuclear Engineering and Technology Programme, Department of Mechanical Engineering, and the third author is with the Department of Electrical Engineering, Indian Institute of Technology Kanpur, Kanpur 208016, India (e-mail: rintu.bhaskar.10@gmail.com; wahi@iitk.ac.in; potluri@iitk.ac.in). Corresponding author: Rintu Bhaskar. Phone: +91-8145667169.

979-8-3315-1721-2/24/$31.00 ©2024 IEEE

Algorithm 1: Reference generator for the FV with the LV's actual trajectory

Initialization: $\mathcal{T} = [\mathcal{T}(1)] = z0$, Trail length = $(n+1)$, $z_{1\text{ref}}(0) = z0$, $z0 := [0,0,0]^T$,$z_{2\text{ref}}(1) = z_2(0)$, and $z_2(0) := [-x_0, 0, 0]^T$; $c(0) = 0$;

/* At $k = 0$, the LV and FV are at standstill at $z0$ and $z_2(0)$, respectively, with a standstill distance of x_0 along the x axis */

while $k > 0$ **do** /* the platoon moves */

$d(k) \triangleq \left\| M[z_1(k) - z_1(k-1)] \right\|_2$, $M \triangleq \begin{bmatrix} 1 & 0 & 0 \\ 0 & 1 & 0 \\ 0 & 0 & 0 \end{bmatrix}$; /* PCVs travel $d(k)$ at an instant */

if $\left\| M[z_{2\text{ref}}(k) - z0] \right\|_2 > 0$ **then** /* FV has not yet reached $z0$ */

$\mathcal{T} := [\mathcal{T}, z_1(k)]$; /* FV stores $z_1(k)$ by padding it to $\mathcal{T}$ */

Find ϵ and $\zeta(k)$ such that

$z_{2\text{ref}}(k) + \zeta(k) = \epsilon z_{2\text{ref}}(k) + (1-\epsilon) z_1(0))$, where $0 \le \epsilon \le 1$ and $\left\| M\zeta(k) \right\|_2 = d(k)$.

update $c(k) = k$; ; /* variable needed for optimization */

else /* FV arrives at $z0$ and travels on trail of LV */

The FV takes n sampling intervals to travel x_0, and at $k = n$ the trail becomes

$\mathcal{T} := [z0, z_1(1), z_1(2), z_1(3), ..., z_1(n)]$;

Update $\mathcal{T}$ by padding $z_1(k)$ and discarding the element of $\mathcal{T}(1)$ as

$\mathcal{T} := [z_1(k-n), z_1(k-(n-1)), z_1(k-(n-2)), ..., z_1(k)]$

Maximize δ such that

$z_{2\text{ref}}(k) + \zeta(k) = \epsilon z_1(k-\delta) + (1-\epsilon) z_1(k-(\delta+1))$,

where $0 \le \delta \le c(k-1)+1$, $0 \le \epsilon \le 1$, $\left\| M\zeta(k) \right\|_2 = d(k)$, and $z_1(k-\delta)$, $z_1(k-(\delta+1)) \in \mathcal{T}$.

update $c(k) = \delta_{\max}$; ; /* $\delta_{\max}$ is obtained from the optimization */

end

$z_{2\text{ref}}(k+1) = z_{2\text{ref}}(k) + \zeta(k)$; /* reference position and orientation of the FV */

$k = k + 1$;

end

the LF and PF topologies. Section III discusses the simulation results. Section IV concludes the paper with a description of possible future work.

II. Algorithmic solution for curved platooning

Consider a platoon consisting of two PCVs to discuss platooning with the LF and PF topologies. A PCV traverses a reference trajectory defined with its reference input position $(x_{\text{ref}}, y_{\text{ref}})$ and orientation (ψ_{ref}) in earth-fixed coordinates. At the k-th sampling instant, a PCV's reference trajectory is represented by $z_{\text{ref}}(k) \triangleq [x_{\text{ref}}(k), y_{\text{ref}}(k), \psi_{\text{ref}}(k)]^T$, and actual trajectory by $z(k) \triangleq [x(k), y(k), \psi(k)]^T$ where, $(x(k), y(k))$ is the position of its center of mass, and $\psi(k)$ is its heading angle from the positive x-axis. The PTC receives the difference between $z_{\text{ref}}(k)$ and $z(k)$ and produces the control input for the PCV. This paper considers the assumptions made in [11]. Initially, at $k = 0$, the LV and the FV are standstill at $z0 \triangleq [0,0,0]^T$ and at $z_20 \triangleq [-x_0, 0, 0]^T$ with a standstill distance of x_0. The following subsections discuss the algorithm.

A. Platooning with Leader-Following Topology

In [11], the FV creates a virtual trail of the LV by storing the LV's communicated reference trajectory $z_{1\text{ref}}$ and the algorithm then finds the FV's reference trajectory $z_{2\text{ref}}$ on that trail. Therefore, in [11], the FV follows the LV's reference trajectory for platooning and remains unaware of the LV's actual position and orientation. To overcome this drawback, in the present work, the LV communicates its actual trajectory $z_1(k) \triangleq [x_1(k), y_1(k), \psi_1(k)]^T$ to the FV, in the k-th sampling interval, and move. The FV stores the communicated $z_1(k)$s as the trail $\mathcal{T}$ of the LV. The algorithm then finds the FV's reference input on that trail using Algorithm 1. This arrangement helps an FV to travel

on the actual path of the LV and not on its reference path as in [11].

The algorithm first finds the FV's reference trajectory on the initial straight line distance x_0 between the initial positions of the LV and the FV for the period τ and then, on the trail of the LV. At each sampling interval, the algorithm calculates the distance d for the FV to travel. In the k-th sampling interval, the distance $d(k)$ can be given as in line 3 of Algorithm 1. At any sampling interval, the LV and FV move the same distance.

While the FV travels on the straight-line distance x_0, it appends $z_1(k)$ on the trail $\mathcal{T}$ at every sampling instant, as in line 5 of Algorithm 1, and the length of $\mathcal{T}$ increases. During this travel on a straight line, the FV's orientation or heading remains unchanged. At the k-th sampling instant, FV's reference position $Mz_{2\text{ref}}(k+1)$ is given by the intersection of the line segment joining $Mz_{2\text{ref}}(k)$ (i.e., FV's reference position) and $Mz0$ (i.e., LV's initial position) with the circle of radius $d(k)$ (i.e., distance to be travelled by the FV) around $Mz_{2\text{ref}}(k)$ as in line 7 of Algorithm 1. The FV's reference input $z_{2\text{ref}}(k+1)$ is then given as in line 19 of Algorithm 1.

During FV's travel on the LV's trail, the length of the trail $\mathcal{T}$ remains fixed. At every sampling instant, FV updates $\mathcal{T}$ by adding $z_1(k)$ at the right of $\mathcal{T}$ and discarding the leftmost element from $\mathcal{T}$, as in line 13 of Algorithm 1. While traveling on the trail of the LV, the FV's reference position $Mz_{2ref}(k+1)$ is given by the intersection of a line segment joining two consecutive points $z_1(k-\delta)$, and $z_1(k-(\delta+1))$ on the LV's trail, and the circle of radius $d(k)$ around $Mz_{2\text{ref}}(k)$ as in line 15 of Algorithm 1. Here, δ represents the index number of the points on the trail starting from the LV's current position, and ϵ represents the ratio of intersection. The intersection also gives the FV's $(k+1)$-th reference heading.

The algorithm solves an optimization problem to find $z_{2ref}(k+1)$, where the objective is to find the point on the trail with the maximum value of δ (i.e., δ_{max}) that corresponds to the closest point, which is $d(k)$ distance away from the FV's current position. For the period τ, the algorithm stores the value of k in variable $c(k)$. Then, it stores the value of δ_{max} in $c(k)$ and uses it in the next sampling interval to ensure that the algorithm always searches the possible δs on the untravelled trail. The work in [11] presents the feasibility of the optimization. Algorithm 1 helps an FV to travel on the LV's actual trajectory. The work in [13] modifies the algorithm for curved platooning under communication losses and delays. This paper assesses the performance of the proposed algorithm in simulation with a platoon of five PCVs.

B. Platooning with Preceding-Following Topology

The paper modifies the algorithm for curved platooning with the PF topology, where the PV communicates its reference and actual trajectory to its immediate FV in two separate approaches. An FV stores the communicated information of its immediate PV as its trail, and the algorithm then finds the reference trajectory of the FV on the trail in both approaches.

1) Preceding Vehicle Communicates its Reference Trajectory for Platooning: In a five-vehicle platoon with the PF topology, the LV communicates its reference position and orientation as $z_{1\text{ref}}(k) \triangleq [x_{1\text{ref}}(k), y_{1\text{ref}}(k), \psi_{1\text{ref}}(k)]^T$ only to the first FV (FV1). The FV1 stores this communicated $z_{1\text{ref}}(k)$ as the LV's trail $\mathcal{T}_1$. The algorithm then finds the reference input $z_{2\text{ref}}(k) \triangleq [x_{2\text{ref}}(k), y_{2\text{ref}}(k), \psi_{2\text{ref}}(k)]^T$ for the FV1 on that trail similar to Algorithm 1. The algorithm first finds the trajectory points for the FV1 on the straight line joining the initial positions of the LV and the FV1. Once the FV1 reaches the initial starting point of the LV, the algorithm finds the trajectory points for the FV1 on the LV's trail $\mathcal{T}_1$.

Then, the first FV communicates to the second FV or FV2 its reference trajectory $z_{2\text{ref}}(k)$. The FV2 stores $z_{2\text{ref}}(k)$ as the trail of its PV (FV1), as $\mathcal{T}_2$, and the algorithm then finds the reference input $z_{3\text{ref}}(k)$ for the FV2 on $\mathcal{T}_2$. Similarly, the FV2 communicates $z_{3\text{ref}}(k)$ to the third FV or FV3, and the algorithm finds the $z_{4\text{ref}}(k)$ for the FV3 from the stored trail of the FV2. Therefore, the communicated information for each FV is different for platooning with PF topology, and each FV creates a separate trail of its PV. Therefore, this paper modifies the Algorithm 1 to consider $z_{i\text{ref}}(k), i \geq 1$ as the communicated information for $(i+1)$-th FV and determine the reference trajectory for that FV. In tracking the PV's reference trajectory, the FV remains unaware of the PV's actual path. To overcome this limitation, this paper investigates curved platooning using the PV's actual trajectory.

2) Preceding Vehicle Communicates its Actual Trajectory for Platooning: The PV communicates its actual position and orientation $z_i(k) \triangleq [x_i(k), y_i(k), \psi_i(k)]^T$ to the immediate FV. The FV stores this communicated information as the trail of its PV. The algorithm then uses this trail and finds the reference position and orientation $z_{(i+1)\text{ref}}(k) \triangleq \left[x_{(i+1)\text{ref}}(k), y_{(i+1)\text{ref}}(k), \psi_{(i+1)\text{ref}}(k)\right]^T$ for the $(i+1)$-th FV. Note that, in this case, the actual trajectory of the PV

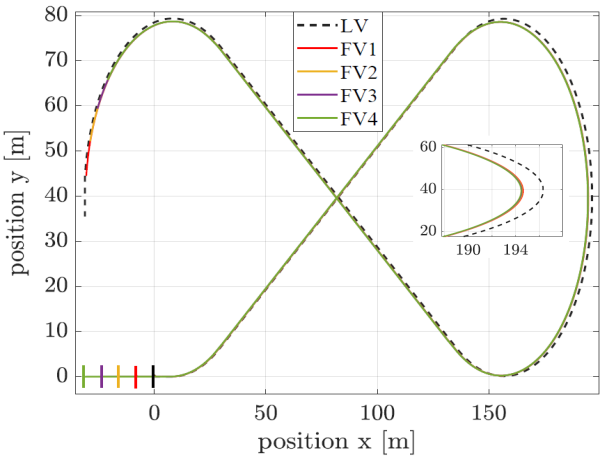


Figure 1: Plots of a platoon of five 4WIS4WID PCVs (with PD as the PTC) traversing a FO8 path with varying speeds and with LV communicating its actual trajectory.

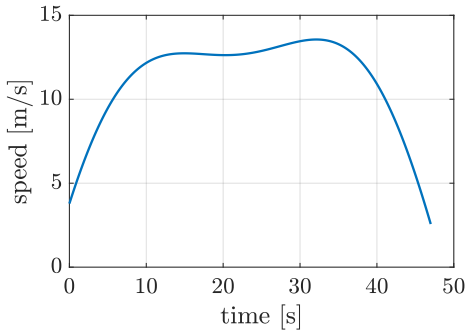


Figure 2: Varying speed $v(t)$ for tracking a FO8 path.

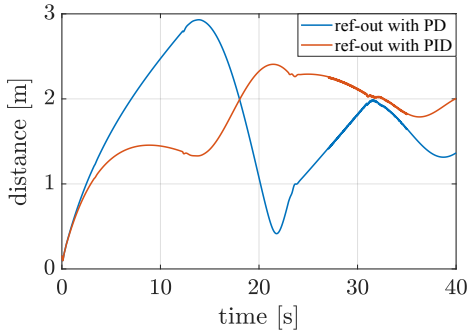


Figure 4: Distance between the reference and actual paths of the 4WIS4WID PCV traversing a FO8 path with PD and PID controllers as the PTC.

becomes the reference trajectory for its immediate FV for platooning. The error in tracking the reference trajectory of the PCV gets added in the platoon from the first FV to the last FV, and the simulation results reflect this error.

III. Simulation Results

This paper considers a platoon of five 4WIS4WID PCVs in simulation for platooning with the LF and PF topologies. In all the simulations, each vehicle starts from a standstill distance of 8 m from its PV with zero lateral offset. In the plots, the black and colored vertical lines on the X-axis represent the starting points of the LV and the FVs, respectively.

A. Curved Platooning with LV's Actual Trajectory

Figure 1 presents the plots of traversing a figure of eight (FO8) path by a platoon of five 4WIS4WID PCVs with varying speeds $v(t)$ as in Figure 2. Here, the LV communicates its actual trajectory. In Figure 1, the actual paths of the FVs (solid-colored lines) coincide but are shifted from the LV's actual path (black dashed line). These shifts are due to PCVs' path-tracking errors, as the LV's actual path is now the reference path for the FVs. Here, the 4WIS4WID PCVs, developed in [12], use a PD controller as the PTC in the form of

$$C_x = C_y = C_\psi \triangleq k_p \frac{T_1 s + 1}{T_2 s + 1},$$

where k_p =1, $T_1 = 100$ and $T_2 = 10$.

This paper designs a PID controller as the PTC for the 4WIS4WID PCV and is given as

$$C_x = C_y = C_\psi \triangleq k_p + k_i \frac{1}{s} + \frac{T_1 s + 1}{T_2 s + 1},$$

where k_p =1, k_i = 0.7, T_1 = 100 and T_2 = 10. This PID controller helps reduce the tracking error between the reference and actual paths of the 4WIS4WID PCV.

Figure 3 shows the reference and actual paths of the 4WIS4WID PCV traversing a FO8 path with the PD and the PID controller as the PTC and with the PID, the path tracking improved. Figure 4 shows the corresponding distance or deviation between the reference and actual paths of the 4WIS4WID PCV in FO8 path traversing. The deviation remains bounded to almost 1 m (1.3 m $<$ deviation $<$ 2.4 m) for most of the path with the PID controller. Whereas with

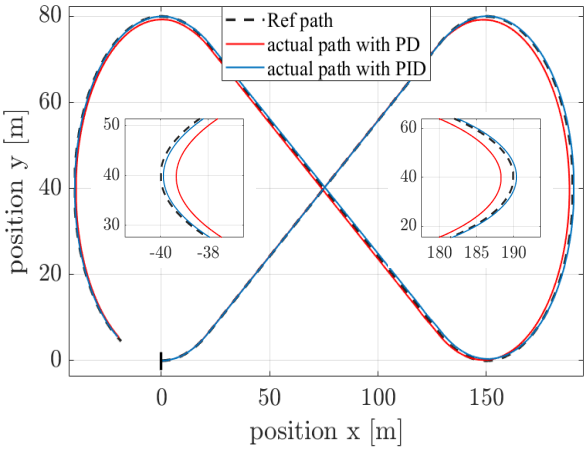


Figure 3: Plots of the reference and output paths of the 4WIS4WID PCV while traversing a FO8 path with PD and PID controllers as the PTC.

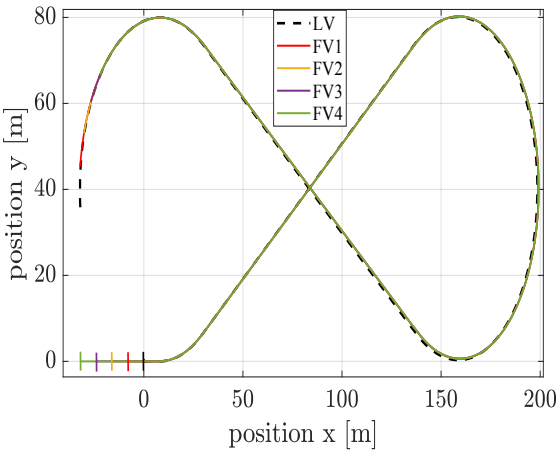


Figure 5: Plots of a platoon of five 4WIS4WID PCVs (with PID as the PTC) traversing a FO8 path with varying speeds and with LV communicating its actual trajectory.

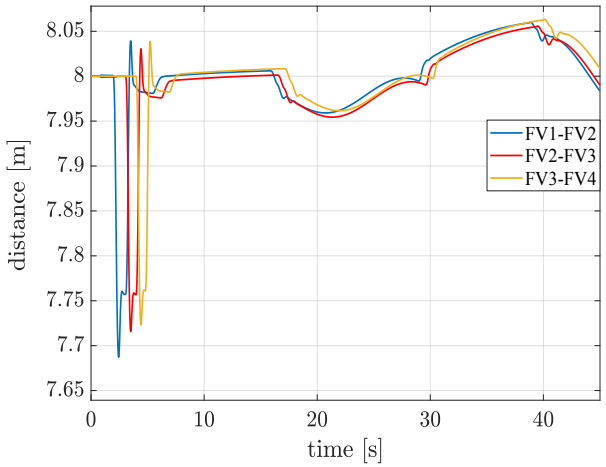


Figure 6: Distance between two successive PCVs in a platoon while traversing a FO8 path with PID as the PTC and the LV is communicating its actual trajectory.

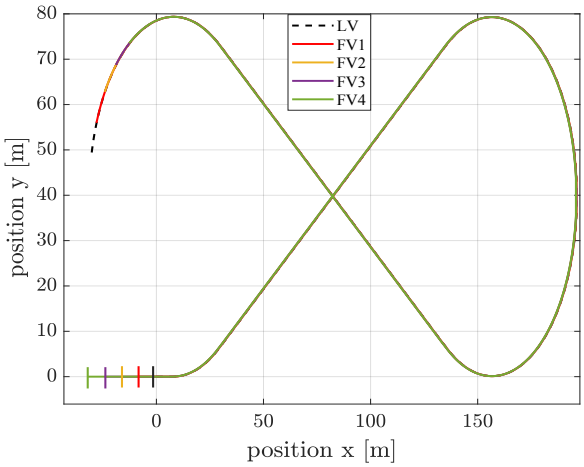


Figure 8: A five-PCV platoon traversing a FO8 path with varying speeds when PV communicating its reference trajectory.

the PD controller, the deviation is more than 2.5 m (0.4 m $<$ deviation $<$ 3.0 m). Therefore, the PID controller reduces the path-tracking error.

Figure 5 presents the plots of FO8 path traversing, with varying speeds, by a platoon of five PCVs (with the PID controller as the PTC). Here, the LV is communicating its actual trajectory for platooning. In Figure 5, the paths of the FVs (solid-colored lines) coincide with the LV's actual path (black dashed line). That is, an FV precisely follows the LV's path. Figure 6 shows the inter-vehicle distance plots between two successive FVs. The error in inter-vehicle distance between the LV and FVs is large (around 13%) due to the error in tracking the LV's actual path as the reference. However, the distance errors between the successive FVs are similar and remain bound to 4 % of the desired distance of 8 m, as shown in Figure 6. Since the inter-vehicle distance errors remain bounded, the platoon can be considered stable. Therefore, the algorithm satisfactorily generates the reference path for the FV when the LV communicates its actual trajectory.

B. Curved Platooning with PV's Reference Trajectory

Figures 7 and 8 present the curved platooning plots with the PF topology where the PV communicates its reference trajectory. Figures 7 and 8 present traversing a circular path at a constant speed and a FO8 path with varying speeds, respectively. In both figures, an FV precisely follows the path of the PV. In both cases, the inter-vehicle distance errors remain bound to 2 % of the desired 8 m distance, and the platoon can be considered stable. Therefore, the algorithmic solution can help achieve satisfactory curved platooning with the PV's communicated reference trajectory.

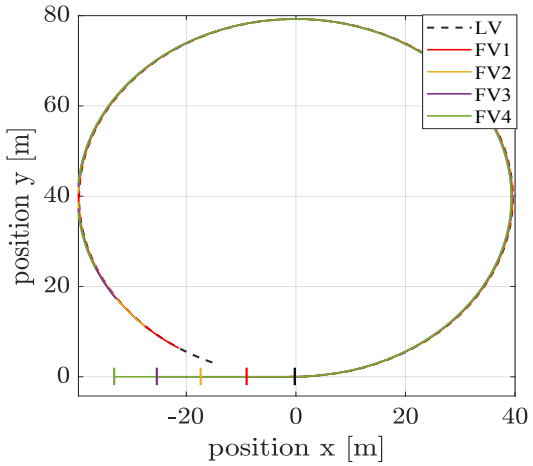


Figure 7: A five-PCV platoon traversing a circular path at a constant speed with PV communicating its reference trajectory.

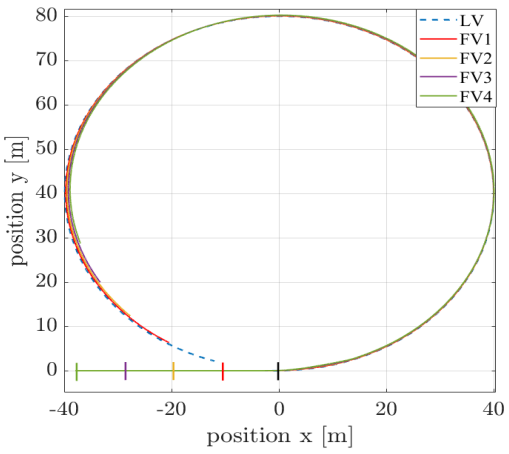


Figure 9: Plots of a platoon of five PCVs (with PID as the PTC) traversing a circular path at a constant speed with PV communicating its actual trajectory.

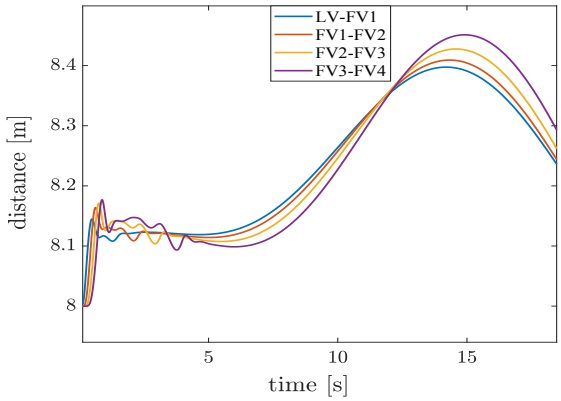


Figure 10: Distance between two successive PCVs in a a platoon while traversing a circular path at a constant speed and with PV's communicated actual trajectory.

C. Curved Platooning with PV's Actual Trajectory

Figure 9 presents the plots of traversing a circular path at a constant speed by a platoon of five PCVs (with the PID controller as the PTC). The PV communicates its actual trajectory. In Figure 9, an FV adequately follows the path of its PV. Figure 10 shows the corresponding inter-vehicle distance errors between two successive vehicles, and the errors are as follows: LV-FV1: 4.97 %; FV1-FV2: 5.11 %; FV2-FV3: 5.35 %, and FV3-FV4: 5.64 % of the desired 8 m distance. The inter-vehicle distance errors are gradually increasing and can cause instability in a large platoon. However, this approach can work for a small platoon of 5 to 10 vehicles.

Figure 11 shows a FO8 path traversing by a five-vehicle platoon with varying speeds and with PV's communicated actual trajectory. An FV can partially follow the FO8 path of the PV as shown in Figure 11, and the inter-vehicle distance errors also increase with platoon length. Therefore, this approach of curved platooning is undesirable.

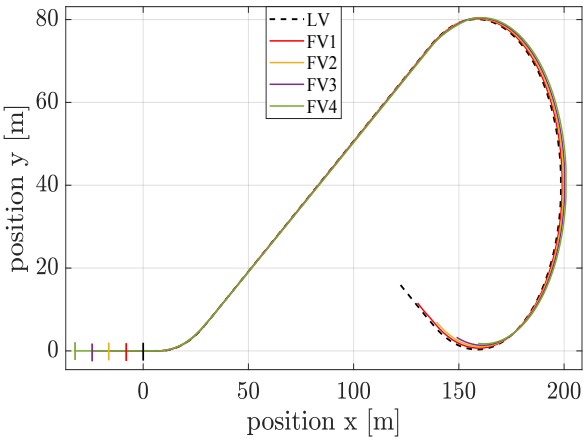


Figure 11: Plots of a platoon of five PCVs (with PID as the PTC) traversing a FO8 path with varying speeds and with PV communicating its actual trajectory.

IV. Conclusion

This paper compares the applicability of the algorithmic solution for curved platooning with LF and PF topologies. The algorithm is modified to use the communicated actual trajectory of the LV and the reference and actual trajectory of the PV to generate the FV's reference path. Platooning with the PV's reference trajectory shows satisfactory performance in simulation. This paper presents a PID controller to reduce the tracking errors in the PTC of the 4WIS4WID PCV for curved platooning with the actual trajectory of the LV and PV. Simulation results suggest satisfactory platooning with the LF topology, but curved platooning can be achieved for a small platoon at a constant speed with the PV's actual trajectory. The incremental inter-vehicle distance can make a large platoon unstable. The use of constant time headway spacing instead of constant distance may overcome the tracking error propagation and can be investigated in future work.

References

[1] P. Seiler, A. Pant, and K. Hedrick, "Disturbance propagation in vehicle strings," *IEEE Transactions on Automatic Control*, vol. 49, no. 10, pp. 1835–1842, 2004.

[2] R. Kianfar, M. Ali, P. Falcone, and J. Fredriksson, "Combined longitudinal and lateral control design for string stable vehicle platooning within a designated lane," in *17th International IEEE Conference on Intelligent Transportation Systems (ITSC)*. IEEE, 2014, pp. 1003–1008.

[3] C. Chang and Z. Yuan, "Combined longitudinal and lateral control of vehicle platoons," in *2017 International Conference on Computer Systems, Electronics and Control (ICCSEC)*. IEEE, 2017, pp. 848–852.

[4] I. Papadimitriou, G. Lu, and M. Tomizuka, "Autonomous lateral following consideration for vehicle platoons," in *Proceedings 2003 IEEE/ASME International Conference on Advanced Intelligent Mechatronics (AIM 2003)*, vol. 1. IEEE, 2003, pp. 401–406.

[5] G. C. Keßler, M. Hakenberg, S. Deutschle, and D. Abel, "Lateral control of heavy-duty vehicle platoons using model-based predictive control1," *IFAC Proceedings Volumes*, vol. 43, no. 7, pp. 791–796, 2010.

[6] T. Fujioka and M. Omae, "Vehicle following control in lateral direction for platooning," *Vehicle System Dynamics*, vol. 29, no. S1, pp. 422–437, 1998.

[7] S. Solyom, A. Idelchi, and B. B. Salamah, "Lateral control of vehicle platoons," in *2013 IEEE International Conference on Systems, Man, and Cybernetics*. IEEE, 2013, pp. 4561–4565.

[8] A. Bayuwindra, J. Ploeg, E. Lefeber, and H. Nijmeijer, "Combined longitudinal and lateral control of car-like vehicle platooning with extended look-ahead," *IEEE Transactions on Control Systems Technology*, vol. 28, no. 3, pp. 790–803, 2019.

[9] S. Wei, Y. Zou, X. Zhang, T. Zhang, and X. Li, "An integrated longitudinal and lateral vehicle following control system with radar and vehicle-to-vehicle communication," *IEEE Transactions on Vehicular Technology*, vol. 68, no. 2, pp. 1116–1127, 2019.

[10] H. Zhao, D. Sun, M. Zhao, Q. Pu, and C. Tang, "Combined longitudinal and lateral control for heterogeneous nodes in mixed vehicle platoon under V2I communication," *IEEE Transactions on Intelligent Transportation Systems*, vol. 23, no. 7, pp. 6751–6765, 2021.

[11] R. Bhaskar, R. Potluri, and P. Wahi, "Reference generator for a platoon of position-controlled vehicles on a curved path," *SAE International Journal of Connected and Automated Vehicles*, vol. 7, no. 12-07-02-0009, 2023.

[12] R. Potluri and A. K. Singh, "Path-tracking control of an autonomous 4WS4WD electric vehicle using its natural feedback loops," *IEEE Transactions on Control Systems Technology*, vol. 23, no. 5, pp. 2053–2062, 2015.

[13] R. Bhaskar, P. Wahi, and R. Potluri, "Platooning of position-controlled vehicles on a curved path under communication losses and delays," *SAE International Journal of Connected and Automated Vehicles*, vol. 7, no. 12-07-04-0028, 2024.